CONFESS

Consistent representation of temporal variations of boundary forcings in reanalyses and seasonal forecasts

Suitable vegetation modelling configuration

Constantin Ardilouze, Gildas Dayon

www.confess-h2020.eu

Co-ordinated by ECMWF

CONFESS

Consistent representation of temporal variations of boundary forcings in reanalyses and seasonal forecasts

D1.3 Suitable vegetation modelling configuration

Author(s): Constantin Ardilouze (MF)
Gildas Dayon (MF)
Fransje van Oorschot (CNR)
Andrea Alessandri (CNR)
Souhail Boussetta (ECMWF)
Gianpaolo Balsamo (ECMWF)

Dissemination Level: Public

Date: 30/04/2023
Version: 0.1
Contractual Delivery Date: 30/04/2023
Work Package/ Task: WP1/ T1.2 and T1.3
Document Owner: Meteo-France
Contributors: MF,CNR,ECMWF
Status: Draft

ECMWF METEO FRANCE CNRM BSC Barcelona Supercomputing Center Centro Nacional de Supercomputación ISAC

CONFESS

Consistent representation of temporal variations of boundary forcings in reanalyses and seasonal forecasts

Research and Innovation Action (RIA)
H2020- LC-SPACE-18-EO-2020 Copernicus evolution: Research activities in support of the evolution of the Copernicus services - Copernicus Climate Change Service (C3S

Project Coordinator: Dr Magdalena Alonso Balmaseda (ECMWF)
Project Start Date: 01/11/2020
Project Duration: 36 months

Published by the CONFESS Consortium

Contact:
ECMWF, Shinfield Park, Reading, RG2 9AX, United Kingdom
Magdalena.Balmaseda@ecmwf.int

The CONFESS project has received funding from the European Union's Horizon 2020 research and innovation programme under grant agreement No 101004156.

Contents

Figures

Tables

1 Executive Summary

Vegetation plays a crucial role in the land surface water and energy balance at the global scale. The availability of good quality Earth observation products covering recent decades together with state-of-the-art modelling capacity provide the unique opportunity to better represent the vegetation and its time evolution in land surface models; and ultimately in coupled models used in climate forecast systems. In the framework of CONFESS, homogeneized high resolution observational datasets of Leaf Area Index (LAI) and Land Cover (LC) have been used to perform and evaluate land surface simulations over the period 1993-2019 with different set-up of vegetation configurations, but a common atmospheric forcing derived from the ERA5 reanalysis. The present document completes the assessment of these simulations provided in the previous deliverable D1.2. , separately for each partner as well as jointly (multi-model approach).

This deliverable takes stock of the full set of simulations to identify the more suitable vegetation configuration to be adopted for seasonal or decadal experiments, as proof of concept of future systems. The main lessons learnt and implications of operational implementation of these developments are provided in the conclusions, which can be summarized as follows:

1) Improvement and careful tuning of land models is needed in order to take advantage of the improved observational datasets. The new observational datasets will help the model development.

2) Temporal variations in LAI have stronger impact on the interannual variations of latent heat and soil moisture than the temporal variations in LC/LU. Because of this, it is expected that in the future, inclusion of prognostic vegetation models will contribute to the skill improvement of seasonal forecasts.

3) The LC/LU datasets from CMIP largely differ from those from ESA-CCI. There is a need for a joint effort towards consistent data sets that can be used for climate simulations, reanalyses and initialized predictions.

2 Introduction

2.1 Background

Vegetation variability at seasonal and inter-annual time scales strongly controls water and energy balances of the land surface. However, state-of-the-art land surface models (LSMs) included in short-term climate prediction systems (e.g. MeteoFrance and ECMWF SEAS5) do not account for sufficiently realistic land cover (LC) and vegetation boundary conditions and do not include parameterizations able to interactively model seasonal to inter-annual variations in vegetation density. Specifically, LC does not change inter-annually in these LSMs, while it is well known to have been changing due to, for example, deforestation or vegetation shifts. Similarly, while the climatological seasonal variations in vegetation density (of which Leaf Area Index, LAI, is a proxy) are described in these LSMs, the inter-annual variations of LAI due, for example, to droughts are not represented. Realistic representations of inter-annual variations in LC and LAI are fundamental to adequately model the signal due to variations in land surface-atmosphere interactions. New observations and latest-generation vegetation data are therefore of paramount importance to properly constrain LSMs used for offline analysis/initialization and for seasonal-to-decadal predictions done with fully coupled climate models.

2.2 Scope of this deliverable

2.3 Objectives of this deliverable

The objective of this deliverable is to provide a comprehensive assessment of the land simulations carried out in the framework of CONFESS WP1 with different vegetation and land-cover configurations, and to draw conclusions about the choice of the most suitable configuration to be used in forecast systems.

2.4 Work performed in this deliverable

The work presented here is primarily concerned with evaluations of offline sensitivity simulations, with a realistic or climatological leaf area index, and a fixed or annually changing land cover. A wealth of details regarding model characteristics and development, reference dataset and experimental setups have been provided in previous deliverables, so they will be described synthetically here, with a cross-reference to those documents if necessary.

2.5 Deviations and countermeasures

No deviations have been encountered.

3 Data and methods

All the experiments carried out in the framework of this work package consist of offline land-only simulations forced by hourly atmospheric fields derived from the ERA5 atmospheric reanalysis (Hersbach et al. 2020) through the common period 1993-2019 (Table 1).

Details about reference datasets and land surface models can be found in Deliverable D1.2. For the sake of clarity, we remind that the DOLCE v3 (Derived Optimal Linear Combination Evapotranspiration version 3) and CLASS (Conserving Land Atmosphere Synthesis Suit) products are used as references for latent heat flux in this document (Hobeichi et al., 2021). The references used for soil moisture (SM) are the So.Mo. (O and Orth, 2021) and ESA-CCI SM (Dorigo et al., 2017, Gruber et al. 2019) products.

Issues have been detected in the Météo France *Ctr* experiment used to produce figures 36 and 37 of Deliverable D1.2. The simulation has been re-run after fixing the issue and the model output files shared among partners (see multi-model analysis in section 4.4 of the present report).

Table 1. Details of experimental setup for CNR, MF and ECMWF models.

Institute	Experiment	Period	Spatial resolution	LAI configuration	Land cover configuration	Effective vegetation cover configuration
CNR	ctr-k5	1993-2019	T255	Climatological (1993-2019)	1993 LC for 1993-2019	k=0.5
	ctr-kv	1993-2019	T255	Climatological (1993-2019)	1993 LC for 1993-2019	k vegetation specific
	pla-k5	1993-2019	T255	Time varying LAI for 1993-2019	1993 LC for 1993-2019	k=0.5
	pla-kv	1993-2019	T255	Time varying LAI for 1993-2019	1993 LC for 1993-2019	k vegetation specific
	plalc-k5	1993-2019	T255	Time varying LAI for 1993-2019	Time varying LC for 1993-2019	k=0.5
	plalc-kv	1993-2019	T255	Time varying LAI for 1993-2019	Time varying LC for 1993-2019	k vegetation specific
MF	eco	1950-2020	T127	Ecoclimap LAI climatology	2000 LC for 1950-2020	
	ctr	1993-2019	T127	Climatological (1993-2019)	2000 LC for 1993-2019	
	pla	1982-2019	T127	Time varying LAI	2000 LC for 1950-2020	
	ila	1950-2020	T127	Dynamic LAI	2000 LC for 1950-2020	
	ila_plc	1950-2020	T127	Dynamic LAI	Time varying LC for 1950-2020 (derived from LUH2)	
ECMWF	ctr	1993-2019	TL639	Climatological (1993-2019)	2019 LC for 1993-2019	
	plc	1993-2019	TL639	Climatological (1993-2019)	Time varying LC for 1993-2019	
	pla	1993-2019	TL639	Time varying LAI for 1993-2019	2019 LC for 1993-2019	
	plalc	1993-2019	TL639	Time varying LAI for 1993-2019	Time varying LC for 1993-2019	

4 Results

In this section, the 3 partners involved provided the latest results from the sets of offline 1993-2019 land simulations with specific vegetation (LAI and land cover) configuration. The last subsection completes the multi-model analysis started in the Deliverable D1.2.

4.1 ECMWF

For ECMWF, the data used in this project is based on the C3S/ESA-CCI LULC and the CGLS LAI. The details of the data processing and homogenisation are shown in Deliverable D1.1.

It is shown that the time varying LULC data is spatially and temporally consistent and suitable for future operational implementation given an appropriate choice of the cross-walking table between the ESA-CCI PFT and the considered model PFT classification. For the time varying LAI (Figure 1) the data is shown to be suitable for use with cautious consideration for the period prior to 1999 over the tropical area, hence 1999-2019 was considered as a reference period.

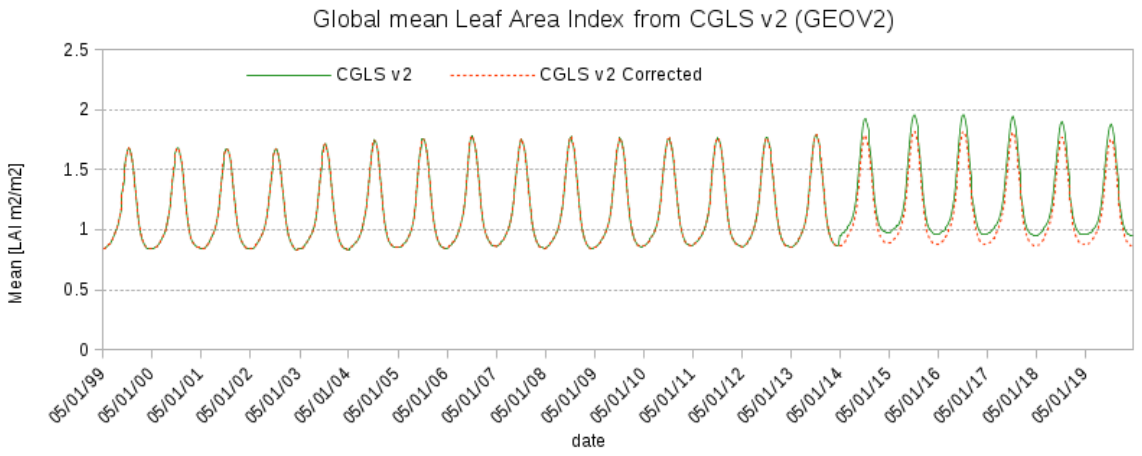

Figure 1. Harmonised global mean CGLS GEOV2 LAI over the 1999-2020 period

When considering LULC data for a recent year (2019) and climatological LAI data based on the 1999-2019 period, the ECMWF system showed mixed positive and negative impacts on surface fluxes and 2m temperature, pointing to the need for further adjustments of the model parameters to suit the new data as it considerably changes the model surface status.

The impact of using time-varying LAI and LULC is evaluated by focusing on both extreme events and long term means of surface latent heat flux and soil moisture. The detailed results corresponding to the different experiments setup (Table 1) are shown in deliverable D1.2. In this document, the main conclusions and recommendations for future developments are presented.

For ECMWF land surface model (ECLand), both Latent heat flux and soil moisture evaluations showed regional differences. The overall skill is, however, marked by a stronger impact when using varying LAI compared to when using varying LULC data only (Figure 2).

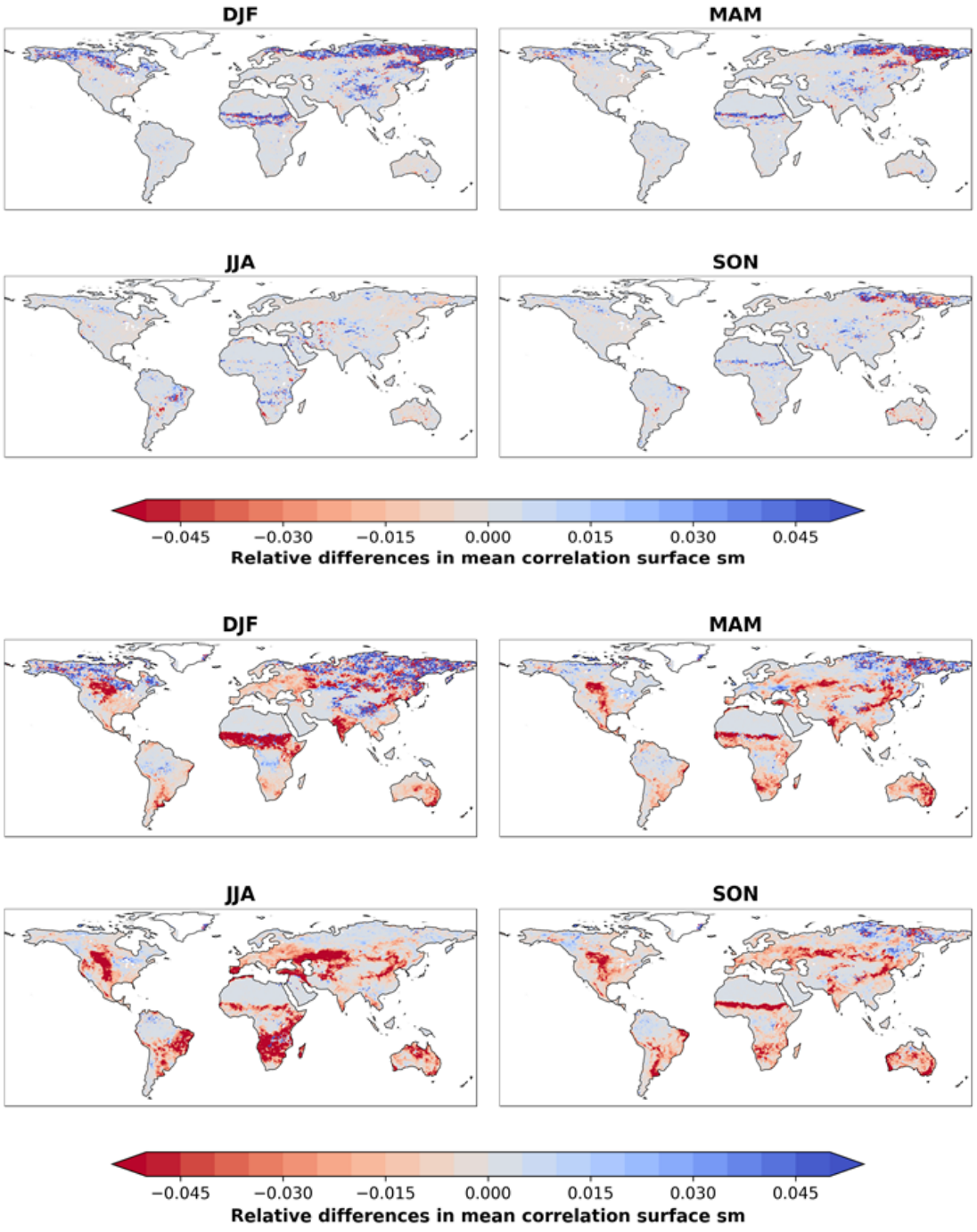

Figure 2: Relative differences in mean correlation for the ECMWF model with regards to the the So.Mo (Sungmin O and R. Orth, 2021) soil moisture data of surface soil moisture anomalies between PLC and CTR simulations (upper panel) and PLA and CTR simulations (lower panel) over the So.Mo period (2000-2019).

The above results were confirmed with the impact on extreme events, which showed more sensitivity to the time varying LAI than the LULC. Although some of the comparisons with different observational based products (FLUXCOM and GLEAM) were conflicting over some regions, the overall outcome was confirmed through the multi-model comparison (section 4.4) and using advanced observational products (CLASS and DOLCE) emphasising the positive impact in better detecting extreme events (Figure 3) when using time-varying vegetation data (mainly LAI).

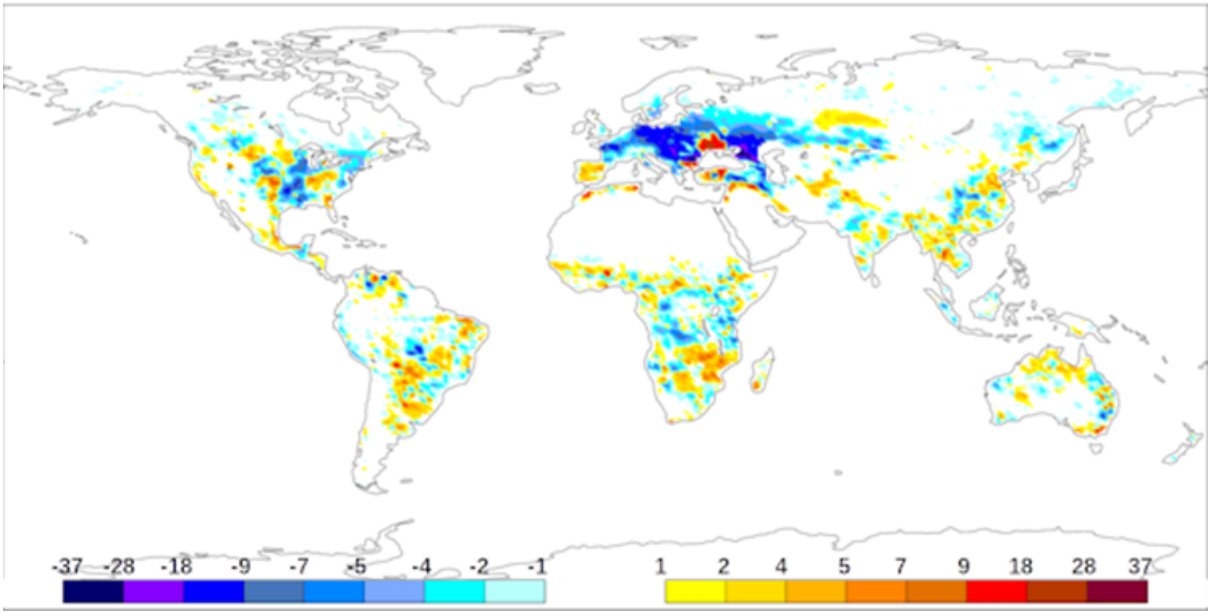

Figure 3. Latent Heat flux absolute bias difference with regards to CLASS data (W/m2) (Hobeichi et al., 2020) between time varying LAI and LULC and control simulation for the European drought (April 2003)

These results triggered new developments within ECLand to better adapt the model parameters to the new LULC and LAI maps and allow operational implementation of these maps as climatological data in a first phase and time varying in a second phase. As a benefit from CONFESS, the results of these developments for the coupled medium range forecast when using the new 2010-2019 climatological LAI and 2019 LULC shows improved atmospheric scores as depicted by the RMSE reduction of the temperature with regards to the ECMWF system's own analysis (Figure 4). These new results consolidate the importance of accurate and up-to-date vegetation data for better coupled atmospheric simulations.

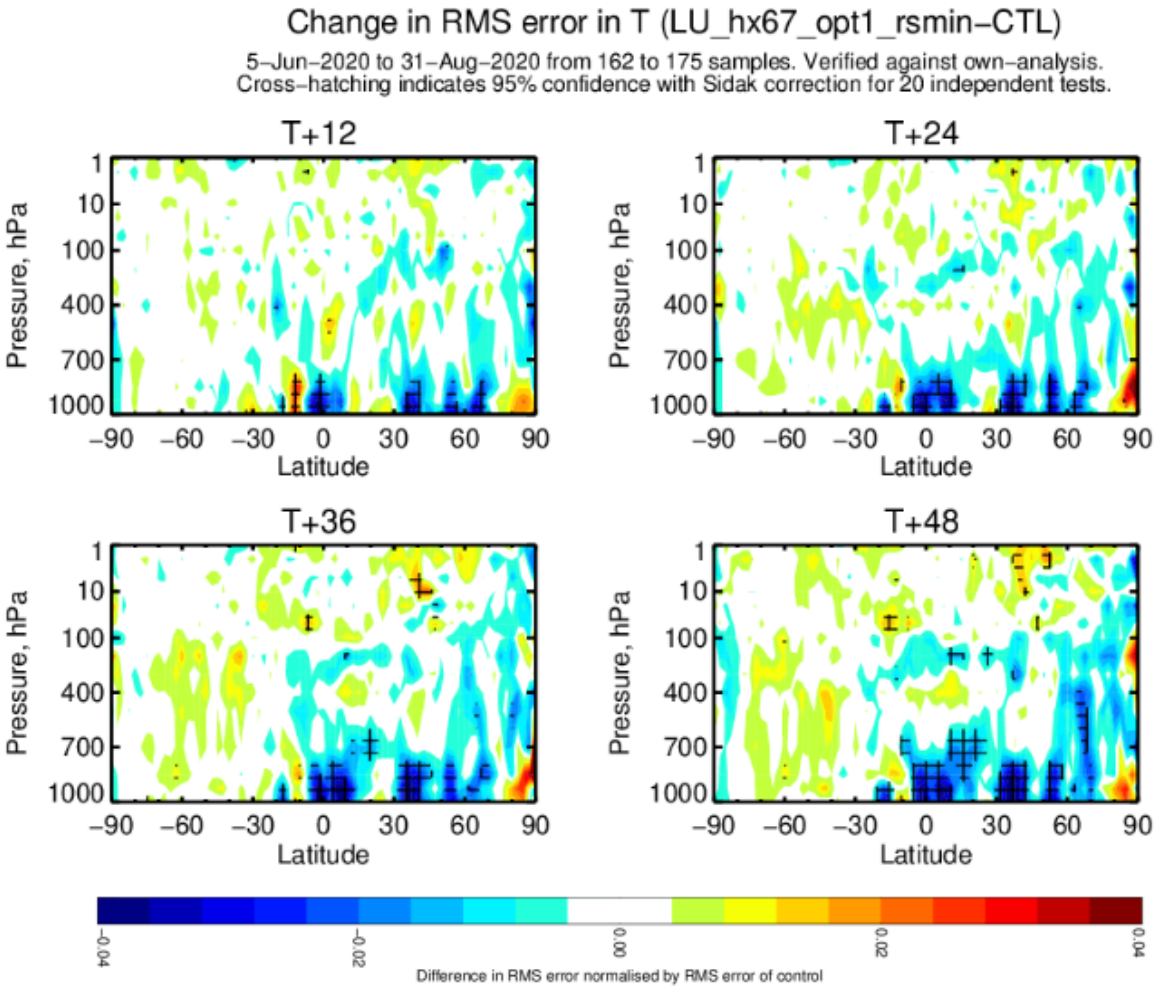

Figure 4. Change in the medium range temperature RMSE with regards to own analysis when using the new 2019 LULC and the 2010-2019 based climatological LAI data (Blue indicates a reduction in the RMSE)

4.2 CNR

The modelling results of CNR models are described in detail in D1.2. Here we provide a summary of the most relevant findings of the different model configurations tested. Figure 5 shows the difference in anomaly correlation of total evaporation (E) and near-surface soil moisture (SMs) between experiments ctr-k5 and plalc-kv (table 1), with respect to DOLCEv3 evaporation and ESA-CCI soil moisture. We found consistent improvements in correlation coefficients for both E and SMs in semiarid regions, during the dry season. These improvements are mostly attributed to the implementation of the inter-annually varying LAI, and inter-annually varying effective vegetation cover (which is a function of LAI). The reduced correlation coefficients for anomaly E in the boreal regions are partly related to a poor fit of the effective vegetation cover parameterization for high LAI values for short grass and tundra (Figure 29 in D1.2). The improved effective vegetation cover parameterization consistently improved the model effective vegetation cover, and regionally improved SMs and E. The inter-annually varying land cover consistently changed the evaporation and

soil moisture in regions with major land cover changes, but the effects were small. All three model developments contribute to an improved representation of vegetation variability, but alter the model land surface states and fluxes differently, with different limitations. Overall, the improved vegetation variability led to improved anomaly correlations of E and SMs improved in 68% and 89% of the land area, respectively. Considering all the results, we conclude that the most suitable vegetation configuration is represented by the plalc-kv experiment that includes all three model developments.

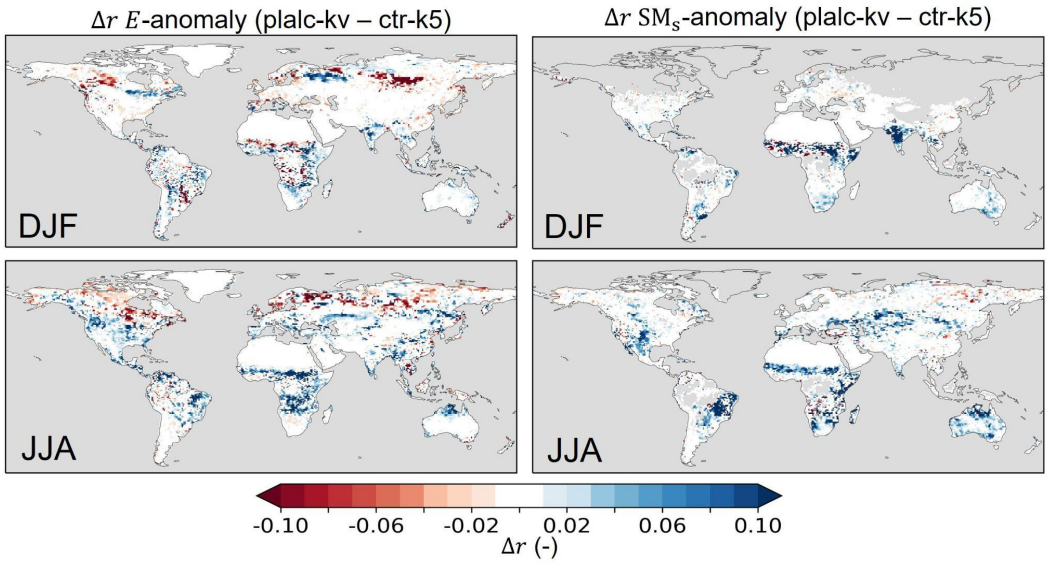

Figure 5. Pearson correlation differences of anomaly evaporation (E) and near-surface soil moisture (SMs) between experiment plalc-kv and ctr-k5 (plalc-kv – ctr-k5) with blue (red) improved (reduced correlations for the seasons DJF and JJA. Reference data for E is DOLCEv3 and for SMs ESA-CCI SM.

4.3 Meteo France

4.3.1 Comparison of land cover datasets and evolution

Unlike the other partners, evolving land-cover (LC) in CNRM simulations is not derived from ESA-CCI but from LUH2 (Hurtt et al, 2020). This configuration was implemented in CNRM-ESM-2 (Séférian et al 2019) with the main objective to properly simulate the carbon cycle and dust emissions.
In CONFESS land-only simulations, we focus on the biophysical impact of evolving LC, prone to feedback on the atmosphere in seasonal predictions.
Note that the LUH2 dataset provides land-use information (as opposed to land-cover) without any assumption on the fraction of bare-soil for example. Hence, the maps shown hereafter do not depict LUH2 directly, but instead the CNRM model vegetation type fractions after disaggregation of LUH2 information into CNRM plant functional types, by means of an automated algorithm.

In the CNRM model, the default fixed LC configuration is called Ecoclimap (Masson et al 2003, Faroux et al, 2013). It is a high-resolution LC map representing vegetation types, rocks and bare soil fraction as well as permanent snow or ice corresponding to the year 2000. In figure 6 are shown the Ecoclimap fractions of high and low vegetation at the resolution of the climate model (left-hand column), and the corresponding fractions for the year 2000 in the evolving LC configuration (middle

column) and in the ESA-CCI dataset after applying regridding and smoothing filters (right-hand column). At first glance, the patterns and fraction ranges look fairly similar, but the differences (Fig. 7) reveal locally important discrepancies. The most striking one is the excessive fraction of low vegetation over the Arabian peninsula in CNRM evolving LC configuration, and the lack of it over south-east Asia. The former issue has been pointed out in Séférian et al (2020) but left as is.

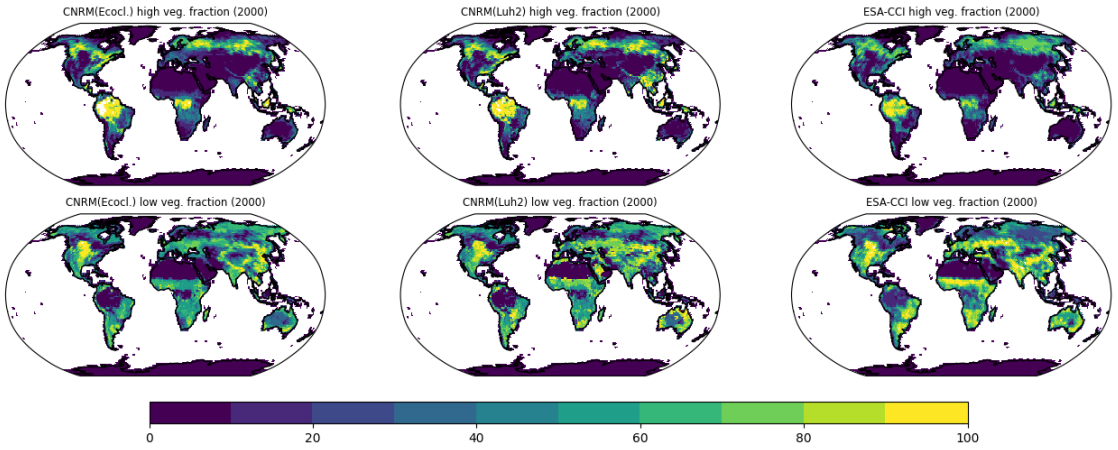

Figure 6 High and low vegetation fraction in 2000 used by ila (left) ila_plc (middle) and ESA-CCI (right)

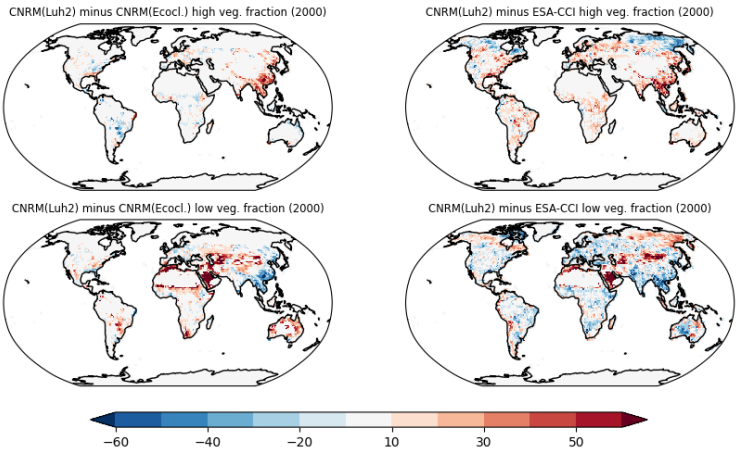

Figure 7 Differences of high and low vegetation fraction in 2000 between those used by ila_plc and (left) ila, (right) ESA-CCI

The compared evolution of low and high vegetation fractions between 1993 and 2019 also show inconsistencies (Fig. 8). Both datasets depict a decrease (increase) in high vegetation fraction over South (North) America but with different amplitude and location. The strong increase in low vegetation fraction in Sahel for CNRM tends to compensate for the lack of it in the year 2000 (Fig. 7 bottom-right). It replaces bare soils in the model, consistently with the overall greening trend of drylands, mentioned in the IPCC special report on Land (cf. Fig 3.6 and associated comments in Shukla et al. 2019)

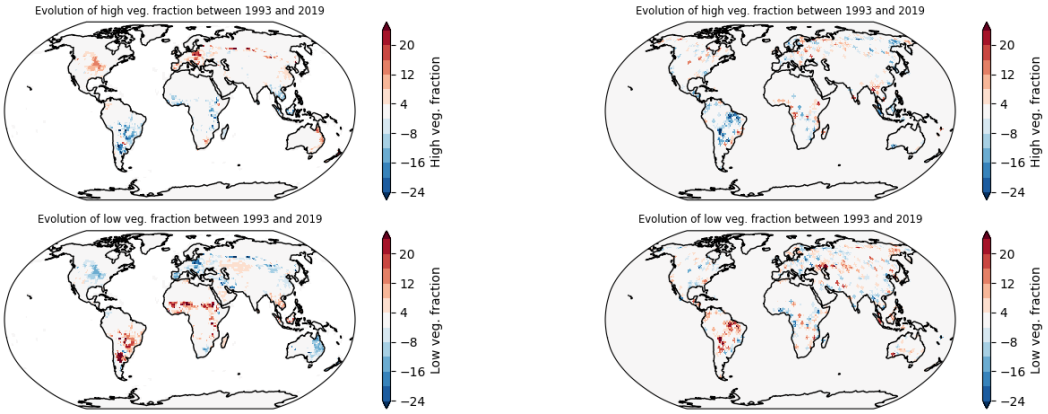

Figure 8 Difference in high and low vegetation fraction between 1993 and 2019 for ila_plc (left) and ESA-CCI (right)

Overall, this comparison of LC maps reveals large differences between datasets and pleads for cautious interpretation of the simulations.

4.3.2 Comparison of offline land simulations with different vegetation configurations

Figure 9 indicates the mean annual bias in latent heat flux for 3 simulations. The model shows consistent positive latent heat flux bias almost everywhere, but considering the uncertainty of the reference dataset and the fact that the simulation is uncoupled, we should not take this overall positive bias for granted. The main interest of this figure is to highlight the very limited impact of vegetation configuration on latent heat flux bias patterns.

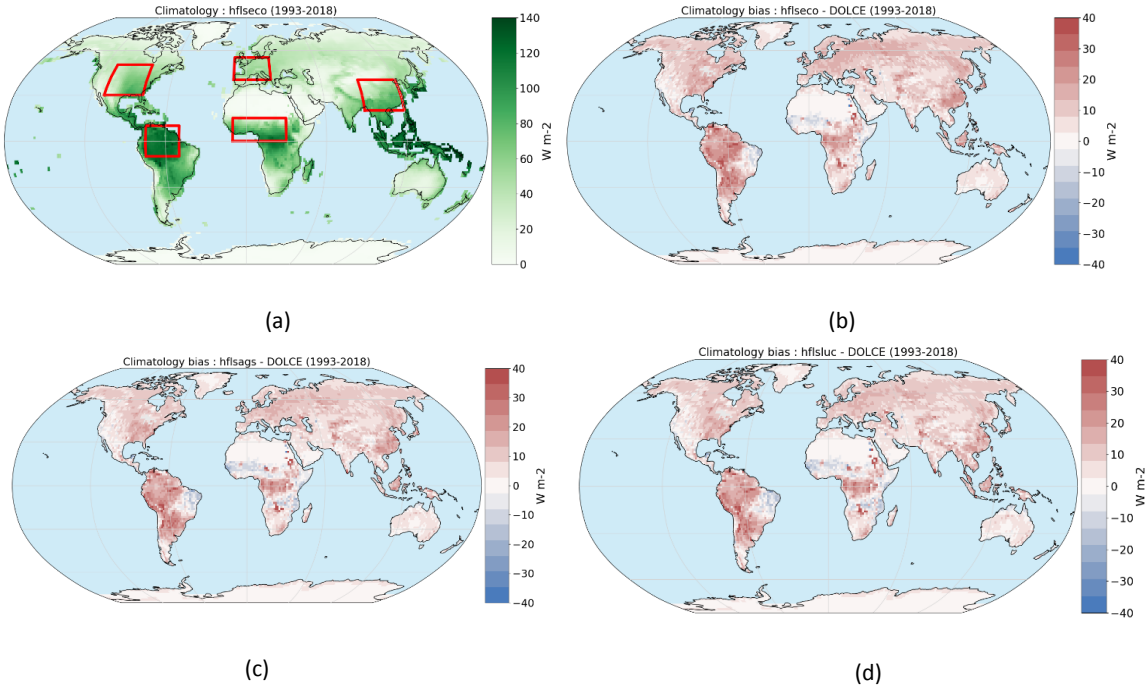

Figure 9: Annual mean latent heat flux in eco (a) and mean bias against DOLCE for eco (b), ila (c) and ila_plc (d), over the 1993-2018 period (Unit: W/m²)

For each grid-point, the correlation of summer (JJA) mean latent heat flux values is computed against the reference DOLCE over the 1993-2018 period. As shown in figure 10, the correlation is fairly high in the eco simulation over relatively dry regions such as western North America, south-east Europe, Australia and Asian steppes, but also humid South-East Asia. The different vegetation configurations all lead to increased correlation over northern hemisphere mid-latitudes. While the simulation pla with prescribed “perfect” LAI does perform better near the equator and northern America, simulations ila and ila_plc with interactive LAI show increased correlation over Europe. The positive impact of evolving LC is noticeable over Argentina, where the fraction of high vegetation decreases throughout the 1993-2018 period (cf. left-hand maps in figure 8). This result is promising in the perspective of considering interannually varying vegetation schemes in forthcoming seasonal forecast systems, but needs to be further consolidated.

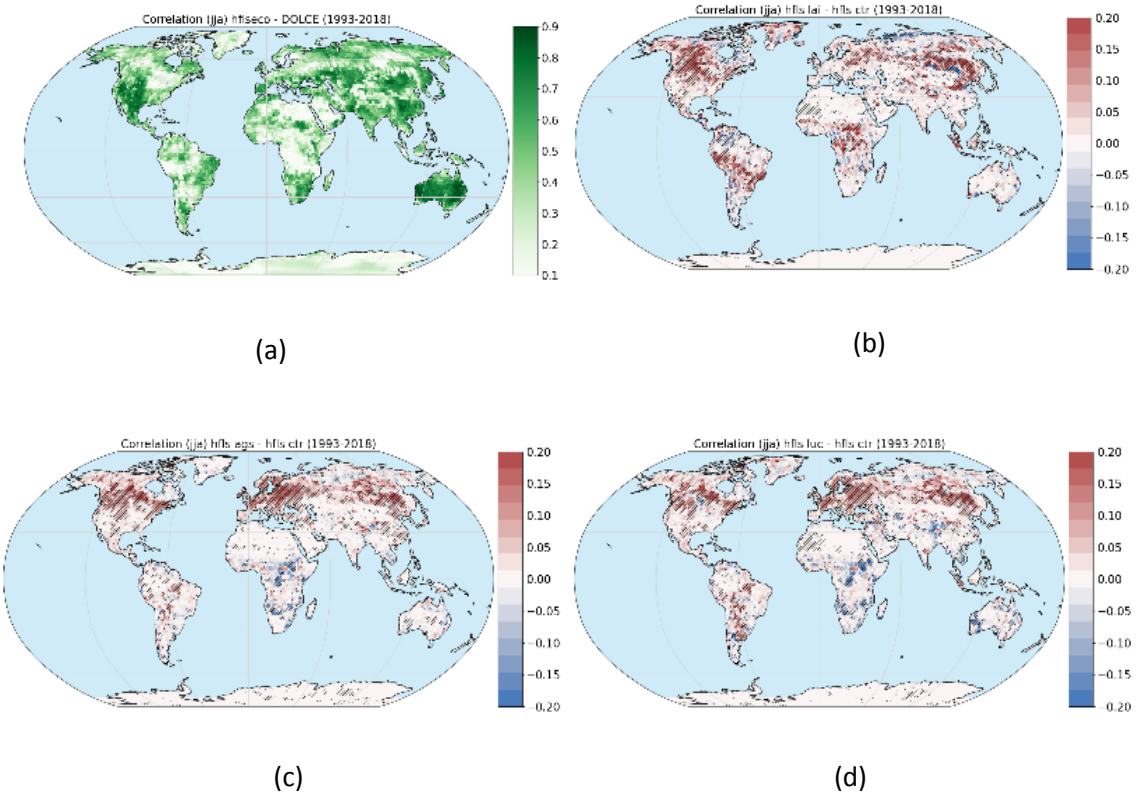

Figure 10: JJA latent heat flux correlation in eco against DOLCE (a) and correlation difference for pla minus eco (b), ila minus eco (c) and ila_plc minus eco (d), over the 1993-2018 period.

The trend in latent heat flux in the eco simulation shows limited agreement with the reference dataset (DOLCE), with particularly strong negative patterns over south-east South America and Central Africa (Fig. 11a-b). Simulations with interactive LAI tend to accentuate these negative patterns although with a spatial shift (Fig. 11c). Evolving land cover (simulation ila_plc) leads to a reduction of the negative trend located over Argentina, eastern Brazil and Sahel, regions where the land cover maps indicate an increase of low vegetation fraction throughout the 1993-2018 period. However, the magnitude of trends in DOLCE and in the Météo France baseline simulation is ~5 times higher than that of trend differences between model simulations with improved vegetation variability and the baseline simulation. This result suggests that the atmospheric forcing predominates the vegetation variability among factors controlling the trend in latent heat flux.

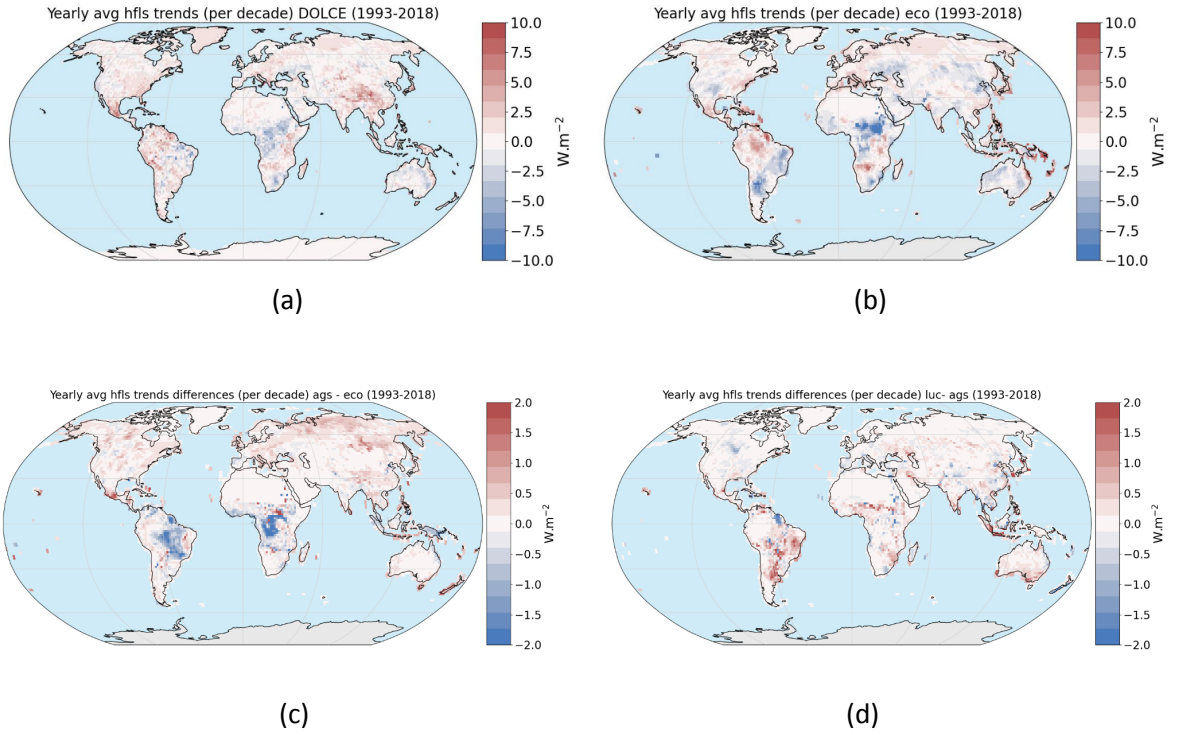

Figure 11: Latent heat flux trend in DOLCE (a), eco(b) and trend difference for ila minus eco (c)) and ila_plc minus ila (d), over the 1993-2018 period (Unit: W/m² per decade)

Hereafter, we evaluate the impact of vegetation configurations on soil moisture climatology, interannual variability and trend.

The global and local seasonal cycles depicted in figure 12 show overall consistency, but with large differences in magnitude. In particular, the magnitude difference between the two references generally exceeds by far the difference between model simulations. In many cases, the simulation with perfect prescribed LAI (pla) has the wettest soils, and eco the driest. Considering the discrepancies between references, and thus the uncertainty of the "true" soil moisture, we cannot draw robust conclusions from the analysis of soil moisture seasonal cycle. In the following analyses, we use a linear combination (arithmetic average) of both GLEAM and ERA5-Land products as the reference (REF) for soil moisture, as in Decharme et al. (2019).

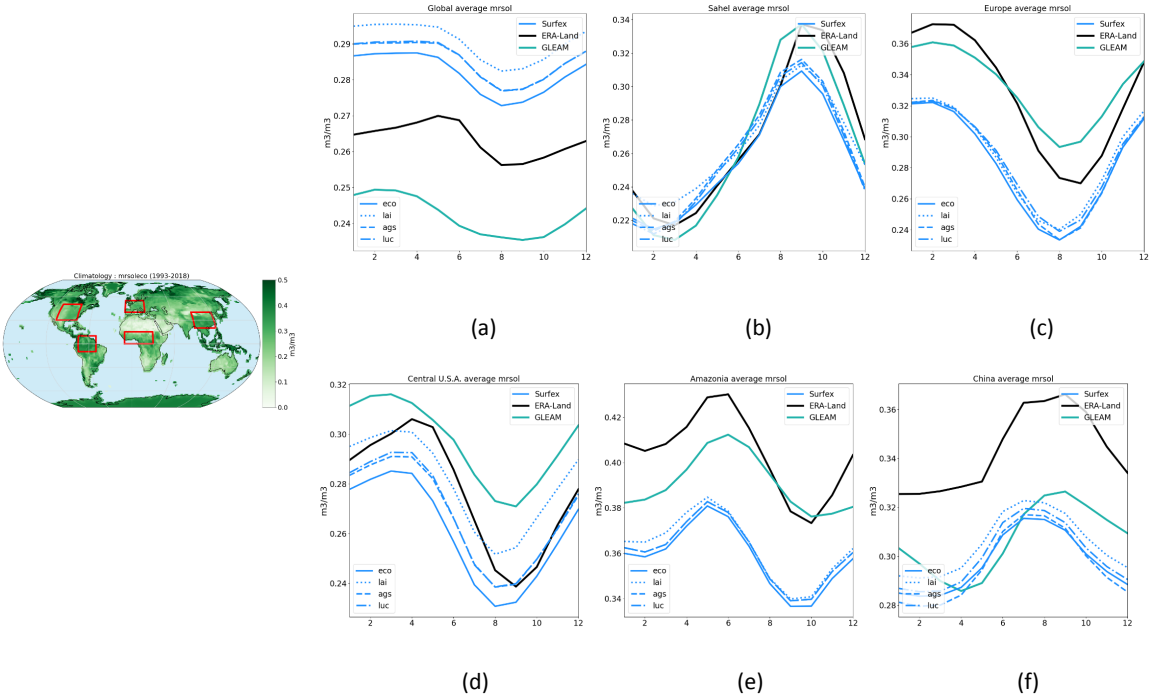

Figure 12: Seasonal cycle of soil moisture (top one-meter depth) at the global scale (a) and over the 5 regions indicated by red boxes on the left-hand map: (b) Sahel, (c) Europe, (d) Central USA, (e) Amazon, (f) China. The green and black lines correspond to GLEAM and ERA5-Land references, respectively. The blue lines correspond to the simulations (solid) eco, (dotted) pla, (dashed) ila and (dash-dotted) ila_plc, over the 1993-2018 period (Unit: m^3/m^3)

Unlike latent heat flux, JJA correlation against REF for soil moisture is high (>0.5) for *eco* over most of the globe, but Sahara desert and northern Amazon where soil moisture variations are weak (Fig. 13a). Simulations with interactive vegetation reveal a decrease of this correlation by up to 0.2 over several regions, in particular Eurasian steppes, southern Africa, Iberian peninsula and Australia. Interestingly, the regions showing a decreased correlation barely overlap with those showing increased correlation in latent heat flux (fig.10 c-d).

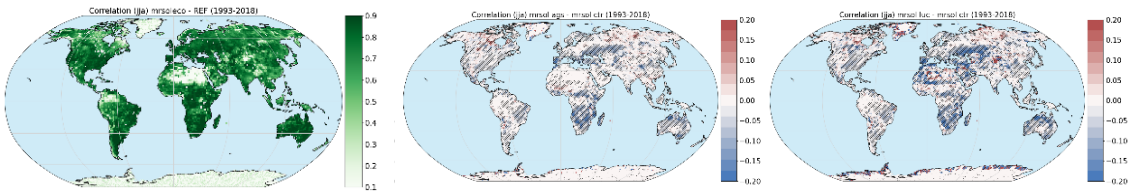

Figure 13: JJA soil moisture correlation in eco against REF (a) and correlation difference for pla minus eco (b), ila minus eco (c) and ila_plc minus eco (d), over the 1993-2018 period.

The trends in soil moisture are relatively consistent for REF and *eco* simulation (Fig. 14a-b), although the strong negative pattern over equatorial Africa mainly results from the spurious decreasing precipitation trend in the meteorological forcing ERA5 (Gleixner et al. 2020). The negative patterns are less pronounced in eco, over central Africa, south America and south-east Europe. Interactive vegetation does not strongly affect soil moisture trends. Evolving land cover (Fig. 14d) impacts the trend in Sahel, consistently with the increase of low vegetation fraction throughout the period. The enhanced evapotranspiration due to crop extension in Sahel explains the increased trend in latent heat flux and decreased trend in soil moisture.

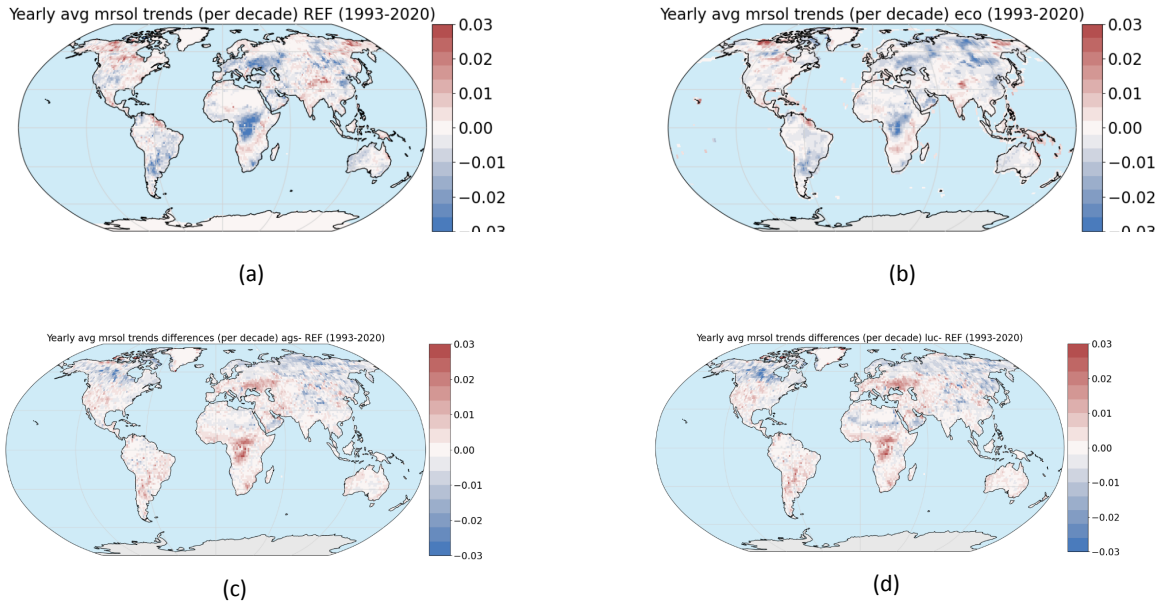

Figure 14: Soil moisture trend in (a) REF, (b) eco, and trend difference for (c) ila minus REF and ila_plc minus REF (d), over the 1993-2018 period (Unit: m^3/m^3 per decade).

Considering all the available results, we advocate pursuing the CONFESS seasonal forecast experiments with the *ila* configuration (interactive vegetation, fixed land-cover). The evolving land cover scheme implemented in the CNRM model bears too much uncertainty and shows excessive discrepancy with ESA-CCI to be used for seasonal forecasts at this stage. Additionally, improving the land cover representation in the CNRM model is a task planned in the time frame of the Horizon Europe CERISE project (2023-2026), ahead of the CMIP7 exercise. The interactive LAI scheme, despite limitations, does not critically degrade the model behaviour. It shows some apparent improvement, yet to be confirmed, in latent heat flux interannual variability over regions without any skill in baseline simulations. Finally, preliminary results from seasonal forecast experiments with initialized and interactive LAI indicate promising skill in LAI anomaly forecast skill. This will be further detailed in the framework of CONFESS WP3.

4.4 Multimodel

Here the multi-model analyses done in D1-2 are further extended. Figure 15 presents the effects of inter-annually varying LAI experiments (sens) on anomaly evaporation and near-surface soil moisture compared to the climatological LAI experiments (ctr). The following experiments are used as control case: ECMWF-ctr, CNR-ctr-kv, and MF-ctr. The sensitivity case is: ECMWF-pla, CNR-pla-kv, and MF-pla (Table 1). The effects of inter-annually varying LAI on evaporation are consistent for the three models, with improved correlation coefficients in semiarid regions with low vegetation and reduced correlation coefficients for the tropics and the boreal regions. On the other hand, the effects on anomaly surface soil moisture are opposite for ECMWF and MF compared to CNR. In all three models, the strongest effects are found in semiarid regions such as the Sahel and the US Great Plains. Here we further elaborate on these opposing results by considering the interactions between soil moisture, vegetation and evaporation.

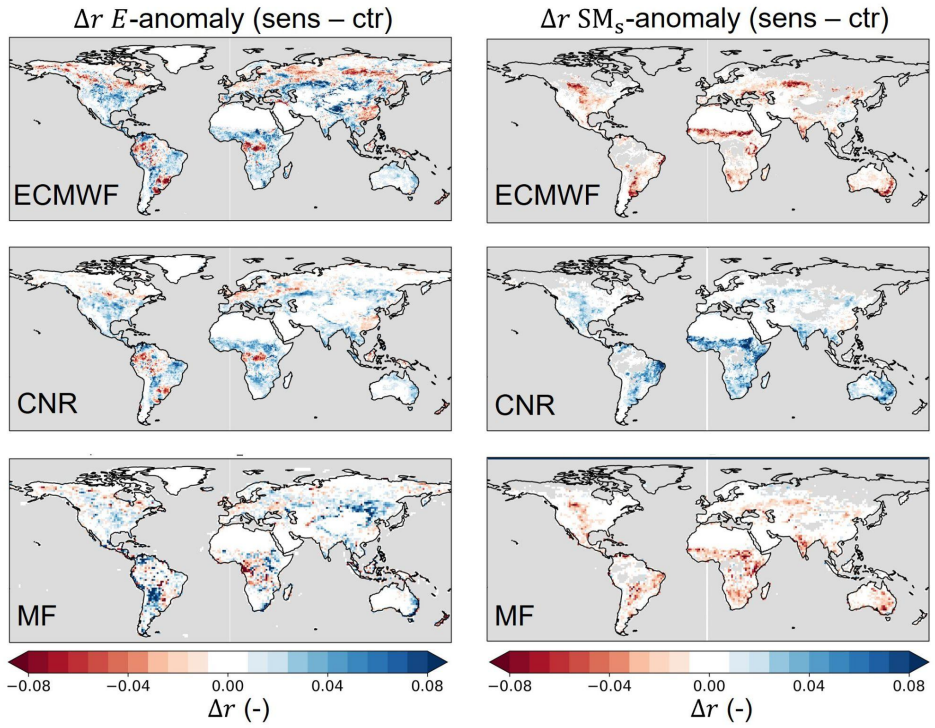

Figure 15. Pearson correlation differences of anomaly evaporation (E) (left) and near-surface soil moisture (SMs) (right) between experiment sens and ctr (sens – ctr) over the 1993-2019 period, with blue (red) improved (reduced) correlations. From top to bottom the correlation differences for ECMWF, CNR and MF models. Reference data for E is DOLCEv3 and for SMs ESA-CCI SM.

The consistently improved correlation coefficients of anomaly near-surface soil moisture with respect to ESA-CCI SM in the CNR model can be explained by the positive feedback presented on the left in Figure 16. During dry periods, soil moisture reduces, which can, in reality, lead to vegetation water stress. In the sensitivity models, this is reflected by a negative LAI anomaly. The reduced LAI leads to a reduced effective vegetation cover, and an increased bare soil cover. As a consequence, soil evaporation increases, which further reduces the near-surface soil moisture in a positive feedback. This feedback is activated with the inter-annually varying LAI in SENS only if the effective vegetation cover is represented as a function of the LAI. In the ECMWF and MF models, the effective vegetation cover is fixed, and the process described on the left in Figure 16 cannot be activated.

In the ECMWF and MF models the negative feedback presented on the right in Figure 16 is dominant. Here, the reduced LAI leads to reduced transpiration, because transpiration is directly a function of the LAI. As a consequence, the negative soil moisture anomaly is dampened through this negative feedback, because less water is extracted. We hypothesize that this negative feedback causes the opposite effects on near-surface soil moisture between the models (Figure 15).

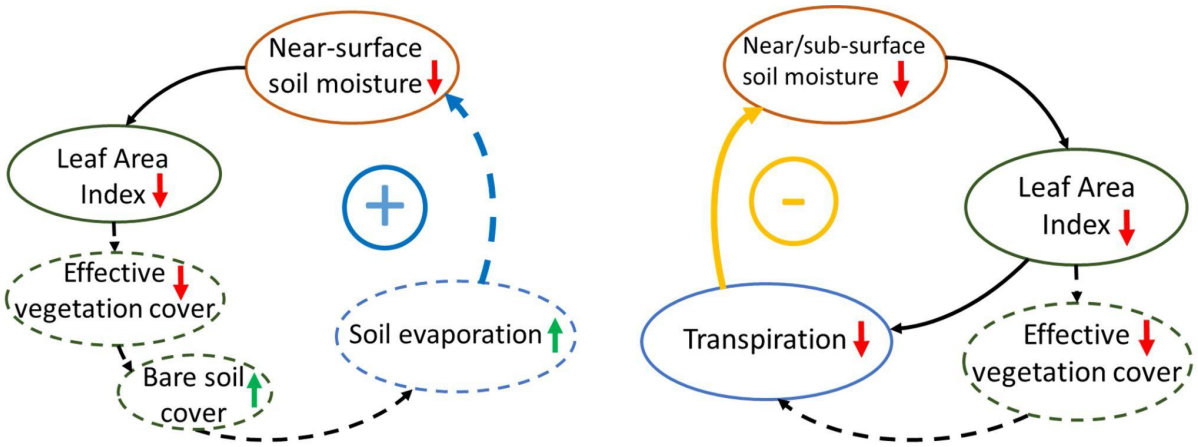

Figure 16. Most dominant vegetation-soil moisture interactions activated with the inter-annually varying LAI in SENS compared to CTR in (left) the CNR model and (right) the MF and ECMWF models. Upward (downward) arrows indicate positive (negative) change in the involved variables. Positive (blue) arrows indicate positive feedback and negative (yellow) arrows indicate negative feedback. +/- refer to the resulting positive/negative feedback loop relative to the sign of the change of the involved variables. Dashed lines are only represented in the CNR model.

Overall, we can conclude from the multi-model evaluation that inter-annually varying LAI is essential to capture variations in evaporation and soil moisture. However, for an adequate representation of the interactions between near-surface soil moisture, vegetation and soil evaporation, the exponentially varying relation between LAI and effective vegetation cover used in the CNR model is needed. The results provide a recommendation for the other modelling groups to integrate a similar representation of the effective vegetation cover as done in the CNR model.

5 Conclusion

The CONFESS WP1 has led to the production and dissemination of homogenized LAI time series and land cover maps spanning the period 1993-2019. These products, among others, have allowed each partner to perform a range of offline land-only simulations with a common atmospheric forcing derived from the ERA5 reanalysis over the same period. The goal was to evaluate the impact of different vegetation set-up concerning the leaf area index, fraction of vegetation cover and spatial distribution of vegetation types.

Results presented in the three WP1 deliverables have allowed each partner to identify the most suitable vegetation configuration to be used in a coupled prediction framework, for skill evaluation before a potential transfer to operations.

The first lesson learnt from these evaluations is that moving forward towards a better representation of vegetation in models needs to be a stepwise process. First attempts to prescribe a more realistic vegetation do not guarantee to improve the model skill, notably because models have been tuned with a baseline climatological vegetation configuration. Thus, models require cautious parameter adjustments to fully benefit from enhanced vegetation configurations, as demonstrated by ECMWF for their ECLand model. Another way forward is to take advantage of the homogenized CONFESS-LAI (see Deliverable D.1) and CGLS-FCover[1] openly available dataset to improve existing parameterizations. By doing so, CNR managed to develop a scheme allowing the fraction of effective vegetation cover to vary as a function of the LAI. They find a major positive impact in terms of soil moisture variability, highlighted by the multi-model comparison.

Another robust conclusion from WP1 results from all partners, is that the impact of evolving land-cover is of lower magnitude than that of inter-annually varying LAI. In the specific case of MF, land cover maps, derived from LUH2 for the CMIP needs, bear strong inconsistencies with ESA-CCI LC maps used by the other partners. An improved strategy to disaggregate LUH2 land use types into adequate plant functional types consistently with ESA-CCI data is now underway. Consequently, unlike CNR and ECMWF, the MF model is not ready to adopt the evolving land cover scheme at this stage.

The interactive LAI scheme tested in the MF model improves the interannual variability of latent heat flux (see also Deliverable D1.2) and mitigates soil moisture depletion during droughts. Due to this positive impact, its usability for real-time forecasts, and promising preliminary results of LAI forecasts, this configuration is the most suitable for MF forecast experiments.

The choice of the most suitable vegetation configuration made by each partner derives mainly (but not only) from the analysis of stand-alone land surface simulations. The coupling with the atmosphere may lead to drastically different model responses (e.g. Laguë et al, 2019) and therefore the model evaluation effort must be pursued to validate the modelling choices. In that respect, the authors recommend that the evaluations of seasonal/decadal hindcasts carried out in the framework of CONFESS be evaluated not only for their prediction skill but also for the bias, variability and trend of forecast atmospheric variables.

[1]Copernicus Global Land Service - Fraction of vegetation Cover

6 References

Dorigo, W., Wagner, W., Albergel, C., Albrecht, F., Balsamo, G., Brocca, L., ... & Lecomte, P. (2017). ESA CCI Soil Moisture for improved Earth system understanding: State-of-the art and future directions. Remote Sensing of Environment, 203, 185-215. https://doi.org/10.1016/j.rse.2017.07.001

Gleixner, S., Demissie, T., & Diro, G. T. (2020). Did ERA5 improve temperature and precipitation reanalysis over East Africa?. *Atmosphere*, *11*(9), 996.

Gruber, A., Scanlon, T., van der Schalie, R., Wagner, W., & Dorigo, W. (2019). Evolution of the ESA CCI Soil Moisture climate data records and their underlying merging methodology. *Earth System Science Data*, *11*(2), 717-739.

Hersbach, H., Bell, B., Berrisford, P., Hirahara, S., Horányi, A., Muñoz-Sabater, J., et al. (2020). The ERA5 global reanalysis. Quarterly Journal of the Royal Meteorological Society, 146(730), 1999–2049. https://doi.org/10.1002/qj.3803

Hobeichi, S., Abramowitz, G., & Evans, J. P. (2021). Robust historical evapotranspiration trends across climate regimes. *Hydrology and Earth System Sciences*, *25*(7), 3855-3874.

Hobeichi, S., Abramowitz, G., & Evans, J. (2020). Conserving land–atmosphere synthesis suite (CLASS). Journal of Climate, 33(5), 1821– 1844. https://doi.org/10.1175/jcli-d-19-0036.1

Hurtt, G. C., Chini, L., Sahajpal, R., Frolking, S., Bodirsky, B. L., Calvin, K., ... & Zhang, X. (2020). Harmonization of global land use change and management for the period 850–2100 (LUH2) for CMIP6. *Geoscientific Model Development*, *13*(11), 5425-5464.

Laguë, M. M., Bonan, G. B., & Swann, A. L. (2019). Separating the impact of individual land surface properties on the terrestrial surface energy budget in both the coupled and uncoupled land–atmosphere system. *Journal of Climate*, *32*(18), 5725-5744.

O, S. and Orth, R. (2021). Global soil moisture data derived through machine learning trained with in-situ measurements. *Scientific Data*, *8*(1), 1-14.

Séférian, R., Nabat, P., Michou, M., Saint-Martin, D., Voldoire, A., Colin, J., ... & Madec, G. (2019). Evaluation of CNRM Earth System Model, CNRM-ESM2-1: role of Earth system processes in present-day and future climate. Journal of Advances in Modeling Earth Systems, 11(12), 4182-4227.

Shukla, P. R., Skea, J., Calvo Buendia, E., Masson-Delmotte, V., Pörtner, H. O., Roberts, D. C., ... & Malley, J. (2019). IPCC, 2019: Climate Change and Land: an IPCC special report on climate change, desertification, land degradation, sustainable land management, food security, and greenhouse gas fluxes in terrestrial ecosystems.

Document History

Version	Author(s)	Date	Changes
	Name (Organisation)	dd/mm/yyyy	
V_0	Constantin Ardilouze (MF) Gildas Dayon (MF)	06/03/2023	Report structure + first results
V_1	Constantin Ardilouze (MF) Gildas Dayon (MF) Fransje van Oorschot (CNR) Andrea Alessandri (CNR) Souhail Boussetta (ECMWF) Gianpaolo Balsamo (ECMWF)	13/04/2023	Finalized results and scope. Submitted to internal review
V_3	Constantin Ardilouze (MF) Gildas Dayon (MF)	28/04/2023	Final version

Internal Review History

Internal Reviewers	Date	Comments
Name (Organisation)	dd/mm/yyyy	
Magdalena Balmaseda (ECMWF)	24/04/2023	
Emanuele Di Carlo (CNR-ISAC)	25/04/2023	See CONFESS_Peer_Review_Form_D1.3_ISAC_CNR_DiCarlo.docx